

Aircrafts' control and command using hierarchical dynamic inversion

MIHAI LUNGU

Avionics Department

University of Craiova

107 Decebal Street, 200440 Craiova

ROMANIA

Lma1312@yahoo.com, mlungu@elth.ucv.ro

<http://www.elth.ucv.ro>

Abstract: - The paper presents a methodology for the flight control law's design for the trajectory pursuit using hierarchical dynamic inversion; this is based on separation of multi-time-scale and multi-loop closing method. The attitude angles are taken as slow variable while angular velocities as fast variables. The slow variables are controlled by the fast ones, which, in turn, are controlled by aerodynamic command surfaces. It greatly simplifies the flight control design compared with PID conventional approaches. The used dynamic equations are classified into 4 groups according to the stairs of time measuring from the physical point of view [1]; each group of variables is controlled by the group of faster neighboring variables. The authors made the analysis of the longitudinal and lateral movements of the aircrafts, have obtained two original block diagrams and, using complex Matlab/Simulink models, have obtained graphic characteristics which demonstrate the effectiveness of the proposed method.

Key-Words: - aircraft, hierarchical dynamic inversion, control law.

1 Introduction

One knows that it is difficult to stabilize and control an aircraft using constant gain controllers because the aircraft's dynamics vary with the considerable modification of the dynamic pressure and Mach number. That's why a very good method for solve this problem is the determination of the gains of the control system. This is a simple and direct methodology for the design of flight control systems. The technique of the gains' determination is the most important thing today in the area of flight control's design [2], [3].

The technique of gains' determination depends on the designer's experience and on his engineering art. Variables' separation on two time scales combined with the theory of singular perturbation have been subject of research, the attitude being taken as slow variable while angular velocities as fast variables. The slow variables are controlled by the fast ones, which, in turn, are controlled by aerodynamic command surfaces.

2 Formulation of the hierarchical dynamic inversion

One considers the following nonlinear system [4], [5], [6], [7], [8], [9], [10]

$$\begin{aligned}\dot{x} &= f(x, u), \\ y &= h(x),\end{aligned}\quad (1)$$

where $x \in R^n$ is the state variable, $u \in R^m$ is the control input and $y \in R^m$ – the output which will be controlled by the control input u . From equations (1), one gets

$$\dot{y} = \frac{\partial h}{\partial x} f(x, u) = F(x, u) \quad (2)$$

or

$$u = F^{-1}(x, v), \quad (3)$$

where v is the auxiliary input of the system. From equations (2) and (3) one yields

$$\dot{y} = F(x, F^{-1}(x, v)) = v. \quad (4)$$

The auxiliary input may have the classical form

$$v = K(y_c - y), \quad (5)$$

where K is a gain matrix and y_c the imposed value of y .

The term that compensates the nonlinear dynamics also provides the linearization of the dynamic system and the exterior loop, expressed by equation (5); the

system becomes linear and achieves the desired value of the output y_c (fig.1).

Unfortunately, some input-output equations do not describe the aircraft dynamics with minimum phase because of the aerodynamic forces' derivatives in rapport with control surfaces' deflections. This fact has prevented the direct application of dynamic inversion to the automatic flight control systems. This problem can be avoided by system's separating on two time scales; thus, there are slow variables and fast variables. Fast state variables are used to control the slow state variables while the fast variables are controlled by the command variable. One considers the following two time scales nonlinear system

$$\dot{x}_1 = f_1(x_1, x_2, u), \dot{x}_2 = f_2(x_1, x_2, u), y = h(x_1), \quad (6)$$

where $x_1 \in R^n$ is the slow state, $x_2 \in R^n$ is the fast state, $u \in R^n$ – the control input and $y \in R^n$ – the controlled output. The input-output equations on the slow scale may be derived as follows

$$\dot{y} = \frac{\partial h}{\partial x_1} f_1(x_1, x_2, u) \equiv F(x_1, x_2, u), \quad (7)$$

where $F(x_1, x_2, u)$ is invertible in rapport with x_2 . One obtains x_{2c} from the previous equation using the dynamic inversion

$$x_{2c} = F^{-1}(x_1, v_1, u), v_1 = K_1(y_c - y), \quad (8)$$

where v_1 is the auxiliary input for the slow scale controller and K_1 – the feedback gain matrix. If $x_2 = x_{2c}$, the following equation is maintained

$$\dot{y} = F(x_1, F^{-1}(x_1, v_1, u)) = K_1(y_c - y) = v_1. \quad (9)$$

Finally, one obtains u_c in the fast scale so that $x_2 \rightarrow x_{2c}$

$$\begin{aligned} u_c &= f_2^{-1}(x_1, x_2, v_2), \\ v_2 &= K_2(x_{2c} - x_2), \end{aligned} \quad (10)$$

where v_2 is the auxiliary input for the fast scale controller K_2 – the feedback gain matrix.

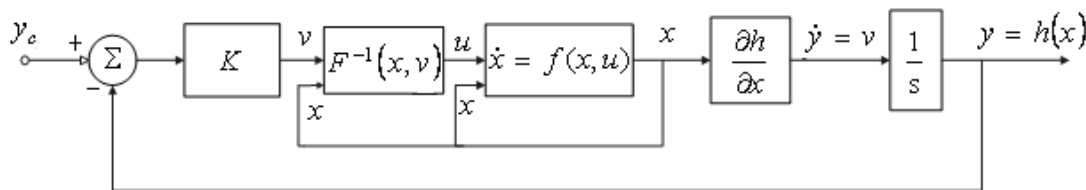


Fig.1 The linear system with dynamic inversion

3 The use of hierarchical dynamic inversion to the aircrafts' dynamics

For the conventional aircrafts with fixed wing the command surfaces' deflections have the slowest time scale [4], [5]. These deflections generate aerodynamic moments around aircrafts' axes. The aerodynamic moments generate angular velocities and the angular velocities are integrated in order to obtain the aircraft's attitude. The forces have the same time scale with the accelerations. The attitude is integrated to obtain the velocities and the velocities give the position of the flying object. The variables may be grouped in four layers (time scales): very slow scale (the position of the aircraft X, Y, Z), slow scale (none of the variables), fast scale (velocities U, V, W and angles φ, θ and ψ) and very fast scale (the angular velocities P, Q, R) [3]. The aircraft position is defined by the longitudinal error e_h , the lateral error e_y and the tra-

jectory arc length s . The velocities are defined by the real velocity of the air currents V_{TAS} , the direction angle in rapport with the air currents ψ_a and the trajectory's angle in rapport with the air currents γ_a . V_{TAS} is directly controlled by the thrust force or by the aerodynamic braking. The attitude is defined by three angles: roll angle φ , pitch angle θ and sideslip angle β ; all these angles are controlled by angular velocities [1]. For the coordinated flight $\beta_c = 0$, the incidence angle α is not considered a state variable as it appears in [3]. This will improve the precision of control because the inertial attitude can be measured with less error than the aerodynamic angles like α . The three angular velocities P, Q, R are controlled by the three command surfaces: rudder, aileron and direction [11], [12], [13]. It is not enough to choose the state variables. This choice may be not optimal for some applications; that's why state transformations will be made.

The state variables are transformed from the initial ones $x \in R^{12}$ in the new state variables $\xi \in R^{12}$. One notes with $T(x)$ the nonlinear transformation which verifies equation $\xi = T(x)$, where ξ is selected so that T – invertible; $x = T^{-1}(\xi)$,

$$x = [X \ Y \ Z \ U \ V \ W \ \varphi \ \theta \ \psi \ P \ Q \ R]^T, \quad (11)$$

$$\xi = [s \ e_y \ e_h \ V_{TAS} \ \psi_a \ \gamma_a \ \varphi \ \theta \ \beta \ P \ Q \ R]^T.$$

The control vector u contains four variables representing the deflections of control surfaces

$$u = [\delta_p \ \delta_e \ \delta_d \ \delta_T], \quad (12)$$

where $\delta_p, \delta_e, \delta_d$ and δ_T are the deflections of the rudder, aileron, direction, respectively the gas lever's displacement. Taking into account the multi time scale separation from the previous section, ξ is separated as follows

$$\xi_1 = [e_y \ e_h], \xi_2 = [V_{TAS} \ \psi_a \ \gamma_a]^T, \quad (13)$$

$$\xi_3 = [\varphi \ \theta \ \beta]^T, \xi_4 = [P \ Q \ R]^T.$$

In layer $i (i = 1,2,3)$ the equations of dynamic models of the subsystems can be defined as

$$\dot{\xi}_i = F_i(\xi_i, \xi_{i+1}, u, \tilde{\xi}_i), \quad i = \overline{1,3}, \quad (14)$$

where $\tilde{\xi}_i$ is a set of state variables other than ξ_i and ξ_{i+1} . On the other hand the dynamic equations of the inner layer ($i = 4$) and those for V_{TAS} are given as

$$\dot{\xi}_4 = F_4(\xi, \delta_T, \tilde{u}), \dot{V}_{TAS} = F_{21}(\xi, \delta_T, \tilde{u}), \quad (15)$$

where \tilde{u} is the set of control variables. This case $\xi_{(i+1)c}, \tilde{u}_c$ and δ_{Tc} are determined from equations [1]

$$x_{(i+1)c} = F^{-1}(x_i, v_i, u, \tilde{x}_i), v_i = K_i(x_{ic} - x_i), \quad (16)$$

$$u_c = f_n^{-1}(x, v_n), v_n = K_n(x_{nc} - x_n).$$

One obtains

$$\xi_{(i+1)c} = F^{-1}(\xi_i, u, \tilde{\xi}_i, v_i), v_i = K_i(\xi_{ic} - \xi_i), \quad (17)$$

$$u_c = F_4^{-1}(\xi, \delta_T, v_4), v_4 = K_4(\xi_{4c} - \xi_4),$$

$$\delta_{Tc} = F_{21}^{-1}(\xi, v_{21}, \tilde{u}), v_{21} = K_{21}(V_{TASc} - V_{TAS}).$$

Using Taylor series expansions of F_i

$$F_i(\xi_i + \Delta\xi, u + \Delta u) \cong F_i(\xi, u) + \frac{\partial F_i}{\partial \xi} \Delta\xi + \frac{\partial F_i}{\partial u} \Delta u \quad (18)$$

and the first equation (17), one gets

$$F_i(\xi_i, \xi_{i+1}, u, \tilde{\xi}_i) + \frac{\partial F_i}{\partial \xi_{i+1}} (\xi_{(i+1)c} - \xi_{i+1}) = K_i(\xi_{ic} - \xi_i), \quad (19)$$

$$F_4(\xi, \delta_T, \tilde{u}) + \frac{\partial F_4}{\partial \tilde{u}} (\tilde{u}_c - u) = K_4(\xi_{4c} - \xi_4),$$

$$F_{21}(\xi, \delta_T, \tilde{u}) + \frac{\partial F_{21}}{\partial \delta_T} (\delta_{Tc} - \delta_T) = K_{21}(V_{TASc} - V_{TAS}).$$

In the above equation the superior order terms have been neglected and that is why the inversion is inexact. Solving equation (19) in rapport with $\xi_{(i+1)c}, \tilde{u}_c$ and δ_{Tc} , one gets

$$\xi_{(i+1)c} = \xi_{i+1} - \left(\frac{\partial F_i}{\partial \xi_{i+1}} \right)^{-1} \{ F_i(\xi_i, \xi_{i+1}, u, \tilde{\xi}_i) - K_i(\xi_{ic} - \xi_i) \}, \quad (20)$$

$$\tilde{u}_c = \tilde{u} - \left(\frac{\partial F_4}{\partial \tilde{u}} \right)^{-1} \{ F_4(\xi, \delta_T, \tilde{u}) - K_4(\xi_{4c} - \xi_4) \},$$

$$\delta_{Tc} = \delta_T - \left(\frac{\partial F_{21}}{\partial \delta_T} \right)^{-1} \{ F_{21}(\xi, \delta_T, \tilde{u}) - K_{21}(V_{TASc} - V_{TAS}) \}.$$

4 Numerical application to the aircrafts' longitudinal movement

One considers the longitudinal movement of an aircraft described by equations [1]

$$[F_1^{lon} \ F_{21}^{lon} \ F_2^{lon} \ F_3^{lon} \ F_4^{lon}]^T = [\dot{e}_h \ \dot{V}_{TAS} \ \dot{\gamma}_a \ \dot{\theta} \ \dot{Q}]^T,$$

$$\begin{bmatrix} \dot{e}_h \\ \dot{V}_{TAS} \\ \dot{\gamma}_a \\ \dot{\theta} \\ \dot{Q} \end{bmatrix} = \begin{bmatrix} a_{11}^{lon} & a_{12}^{lon} & a_{13}^{lon} & a_{14}^{lon} & a_{15}^{lon} \\ a_{21}^{lon} & a_{22}^{lon} & a_{23}^{lon} & a_{24}^{lon} & a_{25}^{lon} \\ a_{31}^{lon} & a_{32}^{lon} & a_{33}^{lon} & a_{34}^{lon} & a_{35}^{lon} \\ a_{41}^{lon} & a_{42}^{lon} & a_{43}^{lon} & a_{44}^{lon} & a_{45}^{lon} \\ a_{51}^{lon} & a_{52}^{lon} & a_{53}^{lon} & a_{54}^{lon} & a_{55}^{lon} \end{bmatrix} \begin{bmatrix} e_h \\ V_{TAS} \\ \gamma_a \\ \theta \\ Q \end{bmatrix} + \begin{bmatrix} b_{11}^{lon} & b_{12}^{lon} \\ b_{21}^{lon} & b_{22}^{lon} \\ b_{31}^{lon} & b_{32}^{lon} \\ b_{41}^{lon} & b_{42}^{lon} \\ b_{51}^{lon} & b_{52}^{lon} \end{bmatrix} \begin{bmatrix} \delta_p \\ \delta_T \end{bmatrix}, \quad (21)$$

$$\xi_{lon} = A^{lon} \xi_{lon} + B^{lon} u_{lon}.$$

The matrices A^{lon} and B^{lon} are the ones from the second equation (21). One customizes the relations (20) for variables $\xi_i (i = \overline{1,4})$ defined by equation (13). Thus, for $i = 1, \xi_{2c}$ has components ψ_{ac}, γ_{ac} and V_{TASc}

$$\xi_{2c}^{lon} = \gamma_{ac} = \gamma_a - \left(\frac{\partial F_1^{lon}}{\partial \gamma_a} \right)^{-1} [F_1^{lon}(\xi_1, \xi_2, u, \tilde{\xi}_1) - v_1^{lon}], \quad (22)$$

where F_1^{lon} verifies equation (14) for $i = 1$; using (21), one obtains

$$\dot{e}_h = F_1^{lon}(V_{TAS}, \gamma_a) = a_{11}^{lon} e_h + a_{12}^{lon} V_{TAS} + a_{13}^{lon} \gamma_a + a_{14}^{lon} \theta + a_{15}^{lon} Q + b_{11}^{lon} \delta_p + b_{12}^{lon} \delta_T \quad (23)$$

and

$$\gamma_{ac} = -(a_{13}^{lon})^{-1} (a_{11}^{lon} e_h + a_{12}^{lon} V_{TAS} + a_{14}^{lon} \theta + a_{15}^{lon} Q) - (a_{13}^{lon})^{-1} [b_{11}^{lon} \delta_p + b_{12}^{lon} \delta_T - K_1^{lon}(e_{hc} - e_h)]. \quad (24)$$

For $i = 2$ one yields [1]

$$\theta_c = -(a_{31}^{lon})^{-1}(a_{31}^{lon} e_h + a_{32}^{lon} V_{TAS} + a_{33}^{lon} \gamma_a + a_{35}^{lon} Q) - (a_{34}^{lon})^{-1}[b_{31}^{lon} \delta_p + b_{32}^{lon} \delta_T - K_2^{lon}(\gamma_{ac} - \gamma_a)] \quad (25)$$

and for $i = 3$ one gets

$$Q_c = -(a_{45}^{lon})^{-1}(a_{41}^{lon} e_h + a_{42}^{lon} V_{TAS} + a_{43}^{lon} \gamma_a + a_{44}^{lon} \theta) - (a_{45}^{lon})^{-1}[b_{41}^{lon} \delta_p + b_{42}^{lon} \delta_T - K_3^{lon}(\theta_c - \theta)] \quad (26)$$

and

$$F_3^{lon} = \dot{\theta} = a_{41}^{lon} e_h + a_{42}^{lon} V_{TAS} + a_{43}^{lon} \gamma_a + a_{44}^{lon} \theta + a_{45}^{lon} Q + b_{41}^{lon} \delta_p + b_{42}^{lon} \delta_T. \quad (27)$$

To calculate \tilde{u}_c the authors use second equation (20), taking into account that $\tilde{u} = [\delta_e \ \delta_p \ \delta_d]^T$. Thus, for the longitudinal movement of the aircrafts, one obtains

$$F_4^{lon} = \dot{Q} = a_{51}^{lon} e_h + a_{52}^{lon} V_{TAS} + a_{53}^{lon} \gamma_a + a_{54}^{lon} \theta + a_{55}^{lon} Q + b_{51}^{lon} \delta_p + b_{52}^{lon} \delta_T, \quad (28)$$

$$\tilde{u}_c^{lon} = \delta_{pc} = \delta_p - (b_{51}^{lon})^{-1}(a_{51}^{lon} e_h + a_{52}^{lon} V_{TAS} + a_{53}^{lon} \gamma_a) - (b_{51}^{lon})^{-1}(a_{54}^{lon} \theta + a_{55}^{lon} Q + b_{51}^{lon} \delta_p + b_{52}^{lon} \delta_T - v_4^{lon}), \quad (29)$$

$$\delta_{pc} = -(b_{51}^{lon})^{-1}(a_{51}^{lon} e_h + a_{52}^{lon} V_{TAS} + a_{53}^{lon} \gamma_a + a_{54}^{lon} \theta) - (b_{51}^{lon})^{-1}[a_{55}^{lon} Q + b_{52}^{lon} \delta_T - K_4^{lon}(Q_c - Q)]. \quad (30)$$

In order to calculate δ_{Tc} one uses the third relation (20). First, F_{21} from equation (21) must be determined

$$F_{21} = \dot{V}_{TAS} = a_{21}^{lon} e_h + a_{22}^{lon} V_{TAS} + a_{23}^{lon} \gamma_a + a_{24}^{lon} \theta + a_{25}^{lon} Q + b_{21}^{lon} \delta_p + b_{22}^{lon} \delta_T, \quad (31)$$

$$\delta_{Tc} = -(b_{22}^{lon})^{-1}(a_{21}^{lon} e_h + a_{22}^{lon} V_{TAS} + a_{23}^{lon} \gamma_a + a_{24}^{lon} \theta) - (b_{22}^{lon})^{-1}[a_{25}^{lon} Q + b_{21}^{lon} \delta_p - K_2^{lon}(V_{TASc} - V_{TAS})]. \quad (32)$$

In general, feedback gains of exterior loop should be smaller than those in the inner loop. As the gains ratio between inner and outer loop is smaller, the interference has less effect and the stability is increased in expense of performance. Therefore the most efficient gain ratio between inner and outer loop is approximately 0.3 to 0.4 [1].

The authors of this paper have increased this ratio to 0.6. This way they increased the stability of the aircraft and its dynamic characteristics. Thus, the loop's gains are

$$\begin{aligned} K_1^{lon} &= (0.6^3) \cdot 1.3 \cdot \pi, \\ K_2^{lon} &= (0.6^2) \cdot 1.3 \cdot \pi, \\ K_3^{lon} &= (0.6^1) \cdot 1.3 \cdot \pi, \\ K_4^{lon} &= (0.6^0) \cdot 1.3 \cdot \pi. \end{aligned} \quad (33)$$

In order to apply the linearised system obtained in the previous section, one uses an ALFLEX aircraft model presented in [1].

In fig.2 the one presents the block diagram that models equations (21), (24), (25), (26), (29) and (32), associated to the longitudinal movement of aircrafts.

Based on this block diagram one obtains the Matlab/Simulink model of longitudinal motion (fig.3) and one will obtains conclusions about the reliability and performance of the control method presented in this paper.

The Matlab/Simulink model from fig.3 has three subsystems: Eq.(25), Eq.(29) and Eq.(32).

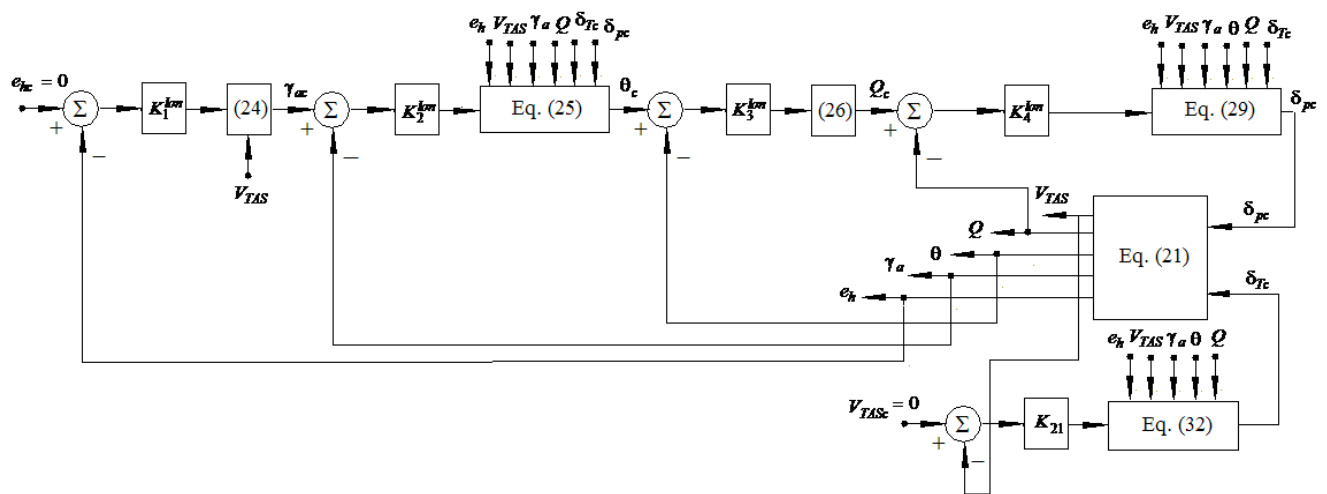


Fig.2 Block diagram of the system for the longitudinal movement's stabilization

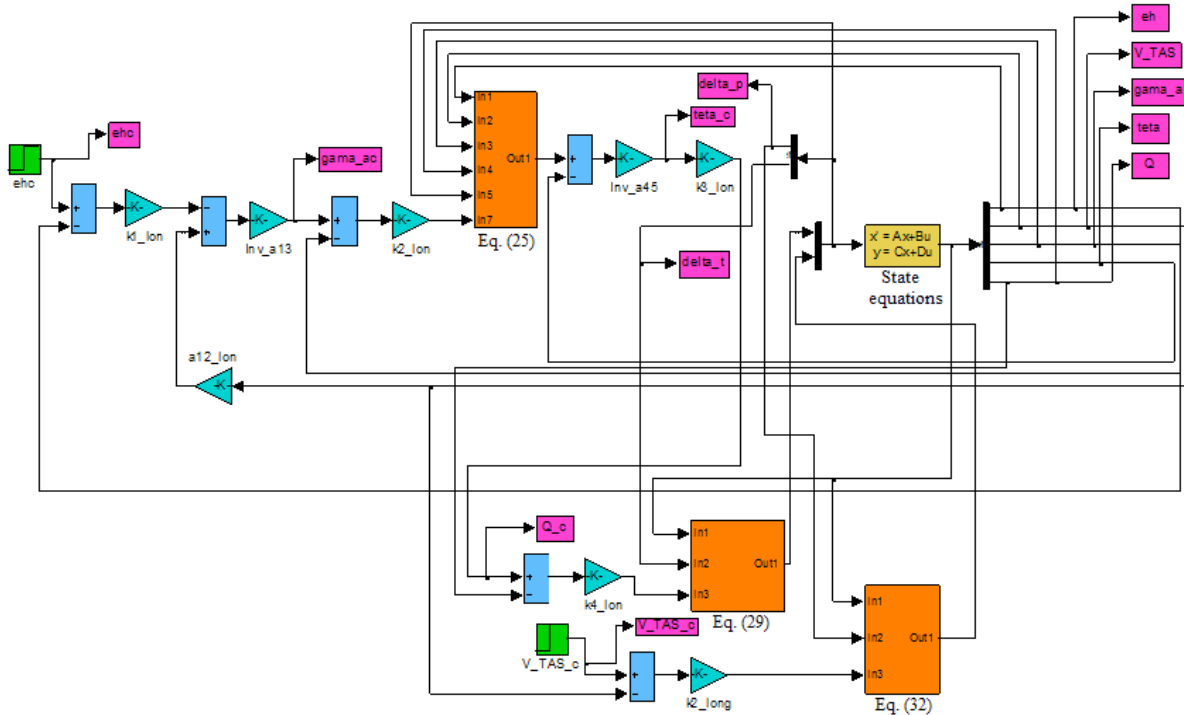


Fig.3 Matlab/Simulink model of the block diagram from fig. 2

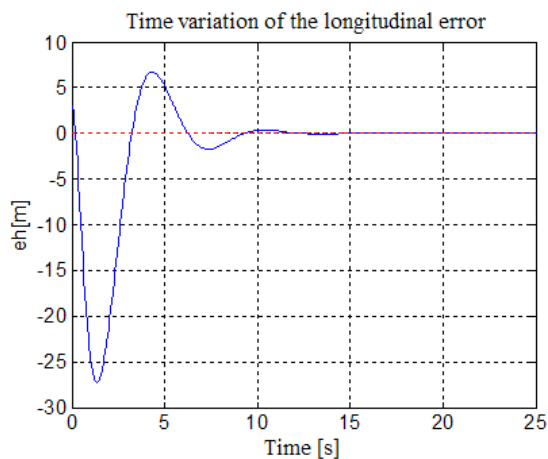


Fig.4 Time variation of the longitudinal error

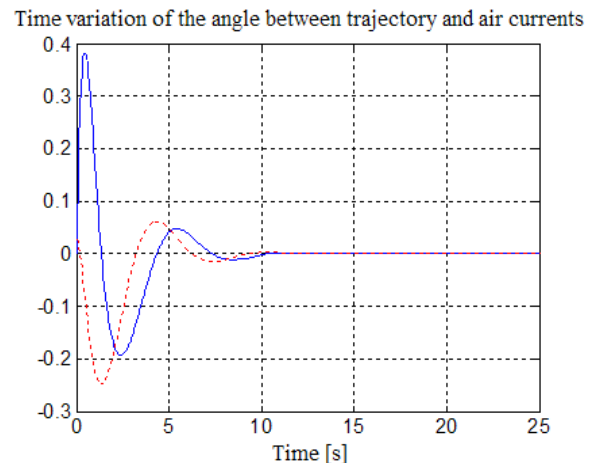


Fig.6 Time variation of the angle between trajectory and air currents

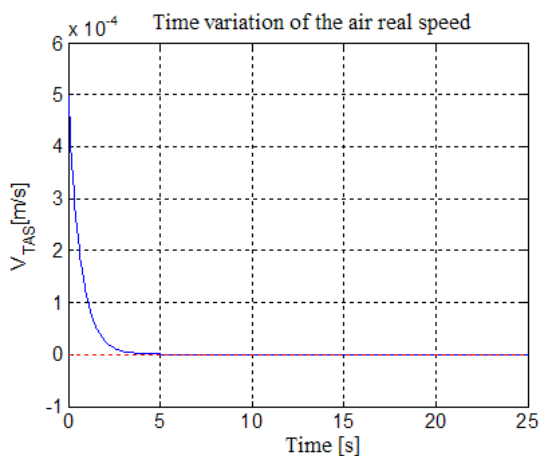


Fig.5 Time variation of the air real speed

Using data for the longitudinal motion, one obtains graphic characteristics representing time variations of the longitudinal error (fig.4), of the air real speed (fig.5), of the angle between trajectory and air current (fig.6), of the pitch angle (fig.7), of the pitch angular velocity (fig.8), of the rudder deflection (fig.9) and of the spoiler deflection (fig.10). In figures 6, 7 and 8 the command variable is represented with red dashed line while the variable (current variable) is represented with blue continuous line. For the simulation one has used the following matrices

$$A^{lon} = \begin{bmatrix} 0 & -0.0392 & -96.907 & 0 & 0 \\ -4.491 \cdot 10^{-5} & -1.0941 & -1.130 & -7.525 & -7.212 \cdot 10^{-6} \\ 9.838 \cdot 10^{-6} & 0.00243 & -1.323 & 1.268 & 4.174 \cdot 10^{-7} \\ 0 & 0 & 0 & 0 & 1 \\ -1.912 \cdot 10^{-7} & -1.037 \cdot 10^{-4} & -1.459 & 1.459 & -1.130 \end{bmatrix},$$

$$B^{lon} = \begin{bmatrix} 0 & 0 \\ -4.596 & -3.216 \\ 0.376 & -0.068 \\ 0 & 0 \\ -14.536 & 2.106 \end{bmatrix}.$$

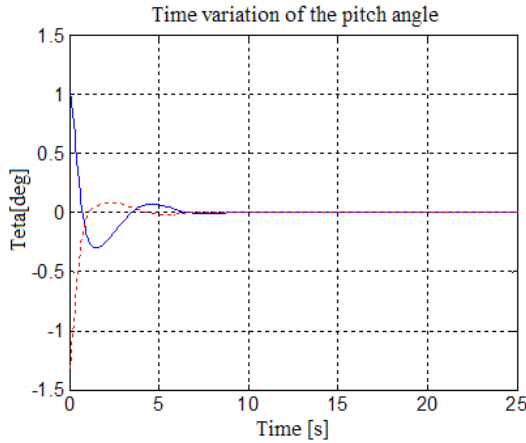


Fig.7 Time variation of the pitch angle

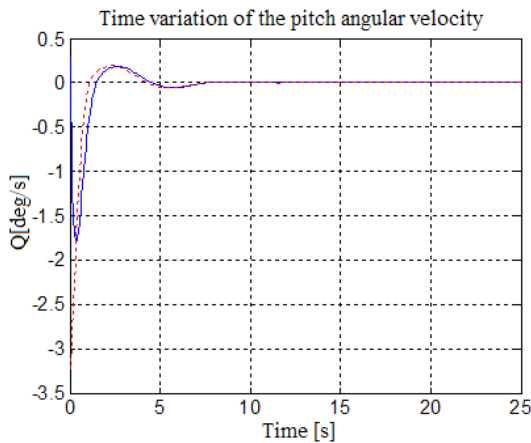


Fig.8 Time variation of the pitch angular velocity

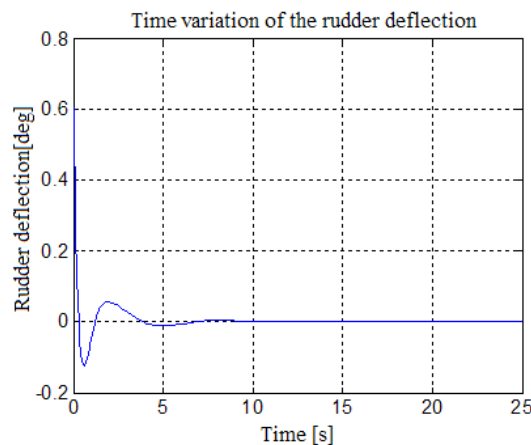


Fig.9 Time variation of the rudder deflection

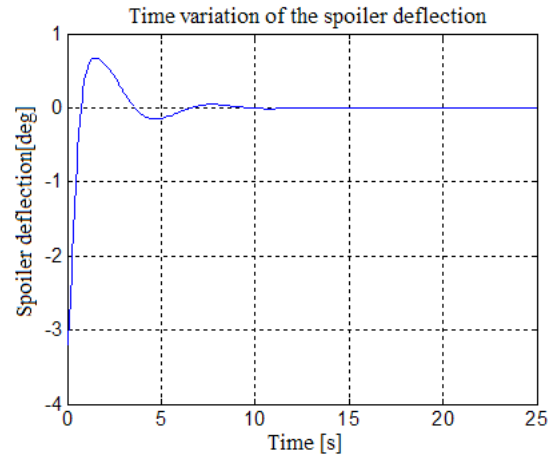


Fig.10 Time variation of the spoiler deflection

5 Numerical application to the aircrafts' lateral movement

One considers the lateral movement of an aircraft described by equations [1], [14]

$$\begin{bmatrix} F_1^{lat} \\ F_2^{lat} \\ F_3^{lat} \\ F_4^{lat} \end{bmatrix} = \begin{bmatrix} \dot{e}_y \\ \dot{\psi}_a \\ \dot{\phi} \\ \dot{\beta} \\ \dot{P} \\ \dot{R} \end{bmatrix} = A^{lat} \cdot \begin{bmatrix} e_y \\ \psi_a \\ \phi \\ \beta \\ P \\ R \end{bmatrix} + B^{lat} \cdot \begin{bmatrix} b_{11}^{lat} & b_{21}^{lat} \\ b_{21}^{lat} & b_{22}^{lat} \\ b_{31}^{lat} & b_{32}^{lat} \\ b_{41}^{lat} & b_{42}^{lat} \\ b_{51}^{lat} & b_{52}^{lat} \\ b_{61}^{lat} & b_{62}^{lat} \end{bmatrix} \begin{bmatrix} \delta_e \\ \delta_d \end{bmatrix},$$

$$A^{lat} = \begin{bmatrix} a_{11}^{lat} & a_{12}^{lat} & a_{13}^{lat} & a_{14}^{lat} & a_{15}^{lat} & a_{16}^{lat} \\ a_{21}^{lat} & a_{22}^{lat} & a_{23}^{lat} & a_{24}^{lat} & a_{25}^{lat} & a_{26}^{lat} \\ a_{31}^{lat} & a_{32}^{lat} & a_{33}^{lat} & a_{34}^{lat} & a_{35}^{lat} & a_{36}^{lat} \\ a_{41}^{lat} & a_{42}^{lat} & a_{43}^{lat} & a_{44}^{lat} & a_{45}^{lat} & a_{46}^{lat} \\ a_{51}^{lat} & a_{52}^{lat} & a_{53}^{lat} & a_{54}^{lat} & a_{55}^{lat} & a_{56}^{lat} \\ a_{61}^{lat} & a_{62}^{lat} & a_{63}^{lat} & a_{64}^{lat} & a_{65}^{lat} & a_{66}^{lat} \end{bmatrix}, B^{lat} = \begin{bmatrix} b_{11}^{lat} & b_{21}^{lat} \\ b_{21}^{lat} & b_{22}^{lat} \\ b_{31}^{lat} & b_{32}^{lat} \\ b_{41}^{lat} & b_{42}^{lat} \\ b_{51}^{lat} & b_{52}^{lat} \\ b_{61}^{lat} & b_{62}^{lat} \end{bmatrix}, \quad (34)$$

$$\xi_{lat} = A^{lat} \xi_{lat} + B^{lat} u_{lat}.$$

One customizes the relations (20) for variables $\xi_i (i = 1,4)$ defined by equation (13). Thus, for the lateral movement of the aircrafts, $i = 1, \xi_{2c}$ has components ψ_{ac}, γ_{ac} and V_{TASc}

$$\xi_2^{lon} = \gamma_{ac} = \gamma_a - \left(\frac{\partial F_1^{lon}}{\partial \gamma_a} \right)^{-1} \left[F_1^{lon}(\xi_1, \xi_2, u, \tilde{\xi}_1) - v_1^{lon} \right], \quad (35)$$

Similar equations are obtained for the lateral movements

$$\psi_{ac} = \psi_a - \left(\frac{\partial F_1^{lat}}{\partial \psi_a} \right)^{-1} \left[F_1^{lat}(\xi_1, \xi_2, u, \tilde{\xi}_1) - v_1^{lat} \right],$$

$$\dot{e}_y = F_1^{lat}(\psi_a) = a_{11}^{lat} e_y + a_{12}^{lat} \psi_a + a_{13}^{lat} \phi + a_{14}^{lat} \beta + a_{15}^{lat} P + a_{16}^{lat} R + b_{11}^{lat} \delta_e + b_{12}^{lat} \delta_d \quad (36)$$

$$\psi_{ac} = -(a_{12}^{lat})^{-1} (a_{11}^{lat} e_y + a_{13}^{lat} \varphi + a_{14}^{lat} \beta + a_{15}^{lat} P + a_{16}^{lat} R) - (a_{12}^{lat})^{-1} [b_{11}^{lat} \delta_e + b_{12}^{lat} \delta_d - K_1^{lat} (e_{yc} - e_y)] \quad (37)$$

For $i = 2$ one yields [1]

$$\beta_c = 0, \varphi_c = \varphi - \left(\frac{\partial F_2^{lat}}{\partial \varphi} \right)^{-1} [F_2^{lat}(\xi_2, \xi_3, u, \tilde{\xi}_2) - v_2^{lat}] \quad (38)$$

where F_2^{lat} is expressed with equation (34) as follows

$$F_2^{lat} = \dot{\psi}_a = a_{21}^{lat} e_y + a_{22}^{lat} \psi_a + a_{23}^{lat} \varphi + a_{24}^{lat} \beta + a_{25}^{lat} P + a_{26}^{lat} R + b_{21}^{lat} \delta_e + b_{22}^{lat} \delta_d \quad (39)$$

$$\varphi_c = -(a_{23}^{lat})^{-1} (a_{21}^{lat} e_y + a_{22}^{lat} \psi_a + a_{24}^{lat} \beta + a_{25}^{lat} P) - (a_{23}^{lat})^{-1} [a_{26}^{lat} R + b_{21}^{lat} \delta_e + b_{22}^{lat} \delta_d - K_2^{lat} (\psi_{ac} - \psi_a)] \quad (40)$$

and for $i = 3$ one gets

$$\begin{bmatrix} P_c \\ R_c \end{bmatrix} = \begin{bmatrix} P \\ R \end{bmatrix} - \left(\frac{\partial F_3^{lat}}{\partial \begin{bmatrix} P \\ R \end{bmatrix}} \right)^{-1} [F_3^{lat}(\xi_3, \xi_4, u, \tilde{\xi}_3) - v_3^{lat}] \quad (41)$$

$$F_3^{lat} = \begin{bmatrix} \dot{\varphi} \\ \dot{\beta} \end{bmatrix} = \begin{bmatrix} a_{31}^{lat} & a_{32}^{lat} & a_{33}^{lat} & a_{34}^{lat} & a_{35}^{lat} & a_{36}^{lat} \\ a_{41}^{lat} & a_{42}^{lat} & a_{43}^{lat} & a_{44}^{lat} & a_{45}^{lat} & a_{46}^{lat} \end{bmatrix} \cdot x + \begin{bmatrix} b_{31}^{lat} & b_{32}^{lat} \\ b_{41}^{lat} & b_{42}^{lat} \end{bmatrix} \begin{bmatrix} \delta_e \\ \delta_d \end{bmatrix} \quad (42)$$

$$\begin{bmatrix} P_c \\ R_c \end{bmatrix} = - \begin{bmatrix} a_{35}^{lat} & a_{36}^{lat} \\ a_{45}^{lat} & a_{46}^{lat} \end{bmatrix}^{-1} \left\{ C \cdot x - \begin{bmatrix} K_{31}^{lat} & 0 \\ 0 & K_{32}^{lat} \end{bmatrix} \left\{ \begin{bmatrix} \varphi_c \\ \beta_c \end{bmatrix} - \begin{bmatrix} \varphi \\ \beta \end{bmatrix} \right\} \right\} \quad (43)$$

where x is the state vector and matrix C has the form

$$C = \begin{bmatrix} a_{31}^{lat} & a_{32}^{lat} & a_{33}^{lat} & a_{34}^{lat} & b_{31}^{lat} & b_{32}^{lat} \\ a_{41}^{lat} & a_{42}^{lat} & a_{43}^{lat} & a_{44}^{lat} & b_{41}^{lat} & b_{42}^{lat} \end{bmatrix} \quad (44)$$

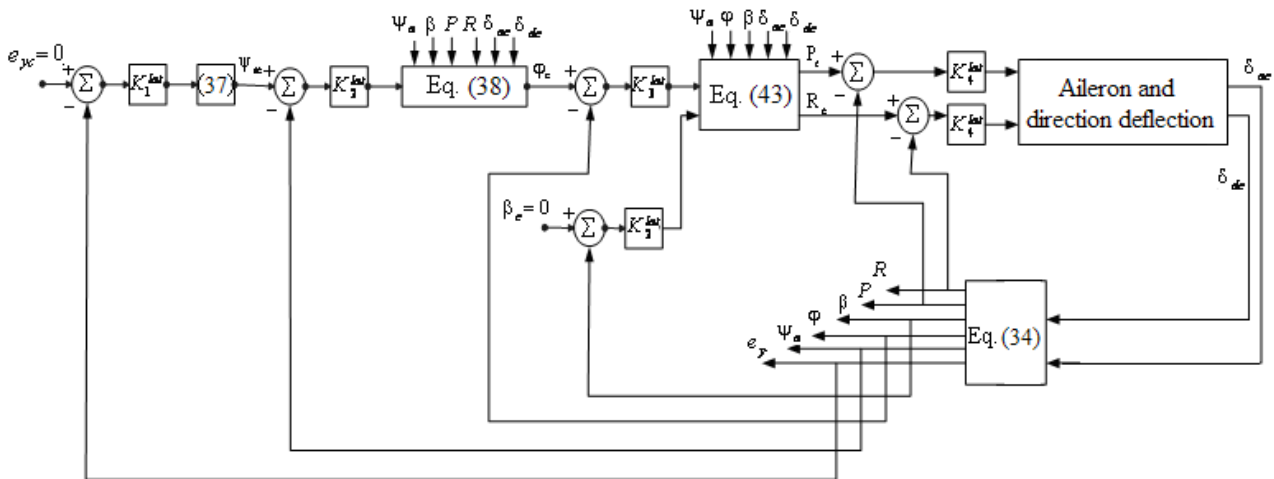


Fig.11 Block diagram of the system for the lateral movement's stabilization

To calculate \tilde{u}_c the authors use second equation (20) and take into account that $\tilde{u} = [\delta_e \ \delta_p \ \delta_d]^T$. Thus, for the lateral movement of the aircrafts, one obtains

$$F_4^{lat} = \begin{bmatrix} \dot{P} \\ \dot{R} \end{bmatrix} = D \cdot x + \begin{bmatrix} b_{51}^{lat} & b_{52}^{lat} \\ b_{61}^{lat} & b_{62}^{lat} \end{bmatrix} \begin{bmatrix} \delta_e \\ \delta_d \end{bmatrix} \quad (45)$$

$$\tilde{u}_c^{lat} = \begin{bmatrix} \delta_{ec} \\ \delta_{dc} \end{bmatrix} = \begin{bmatrix} \delta_e \\ \delta_d \end{bmatrix} - \left(\frac{\partial F_4^{lat}}{\partial \begin{bmatrix} \delta_e \\ \delta_d \end{bmatrix}} \right)^{-1} [F_4^{lat}(\xi, \delta_r, \begin{bmatrix} \delta_e \\ \delta_d \end{bmatrix}) - V_4^{lat}] \quad (46)$$

with

$$D = \begin{bmatrix} a_{51}^{lat} & a_{52}^{lat} & a_{53}^{lat} & a_{54}^{lat} & a_{55}^{lat} & a_{56}^{lat} \\ a_{61}^{lat} & a_{62}^{lat} & a_{63}^{lat} & a_{64}^{lat} & a_{65}^{lat} & a_{66}^{lat} \end{bmatrix} \quad (47)$$

The most efficient gain ratio between inner and outer loop is approximately 0.3 to 0.4 [1]. The authors of this paper have increased this ratio to 0.5 [14]. This way they increased the stability of the aircraft's lateral movement and its dynamic characteristics. Thus, the loop's gains are

$$K_1^{lat} = (0.5^3) \cdot 1.3 \cdot \pi, K_2^{lat} = (0.5^2) \cdot 1.3 \cdot \pi, K_3^{lat} = (0.5^1) \cdot 1.3 \cdot \pi, K_4^{lat} = (0.5^0) \cdot 1.3 \cdot \pi \quad (48)$$

Same ALFLEX aircraft model presented in [1] has been chosen for simulations. In fig.11 one presents the block diagram that models equations (34), (37), (38), (43) and (46), associated to the lateral movement of aircrafts. The Matlab/Simulink of the block diagram is the one from fig.12. The Matlab/Simulink model from fig.12 has three subsystems: Eq. (38), Eq.(43) and Eq.(46).

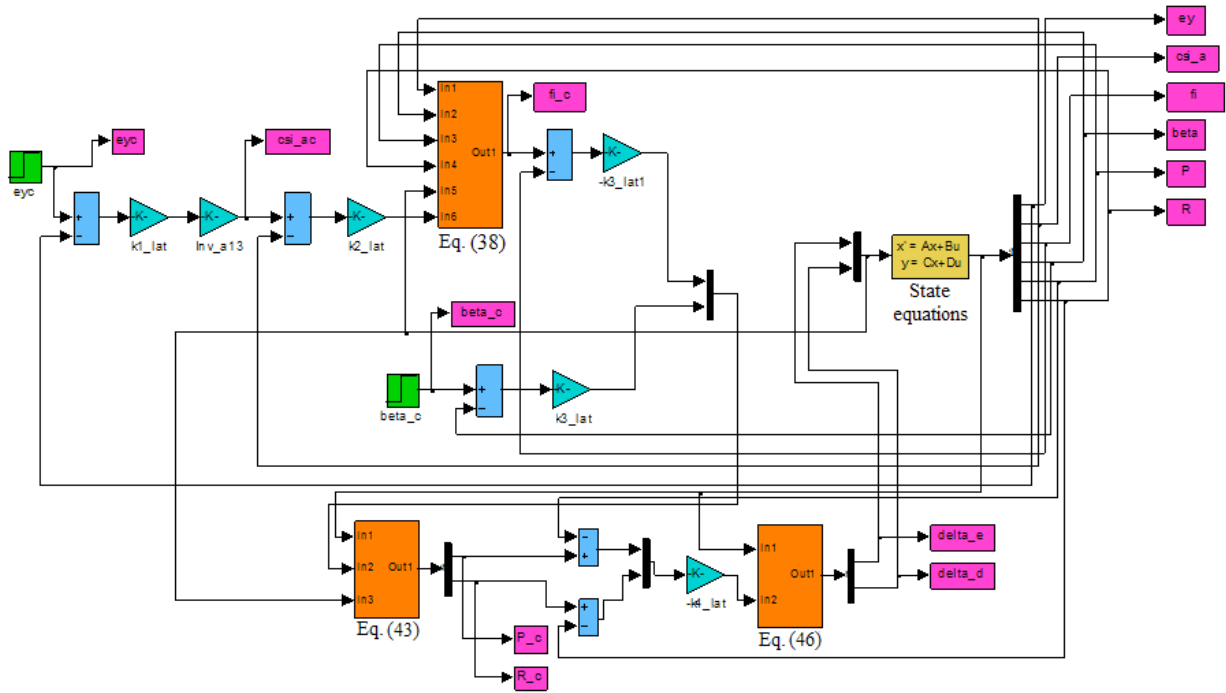


Fig.12 Matlab/Simulink model of the block diagram from fig.11

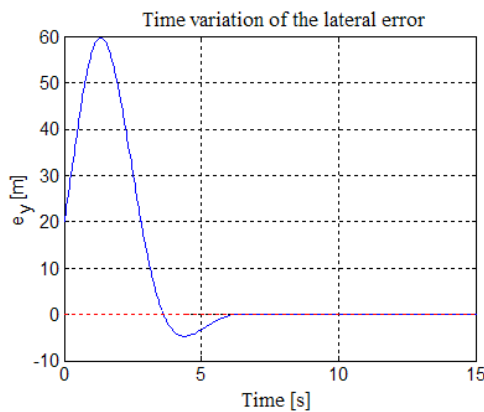


Fig.13 Time variation of the lateral error

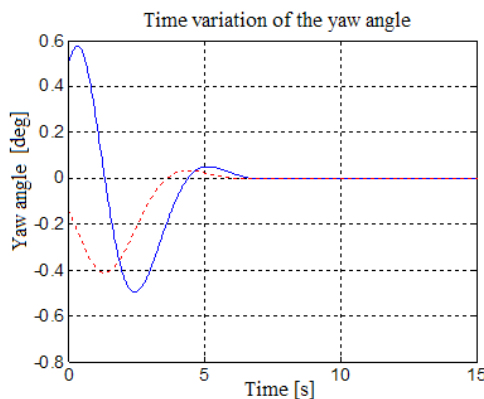


Fig.14 Time variation of the yaw angle

Next, using data for the lateral motion, one obtains graphic characteristics representing time variations of the lateral error (fig.13), yaw angle (fig.14), roll angle (fig.15), aileron deflection (fig.16) and direc-

tion deflection (fig.17). In figures 14 and 15 the command variable is represented with red dashed line while the variable (the current variable) is represented with blue continuous line.

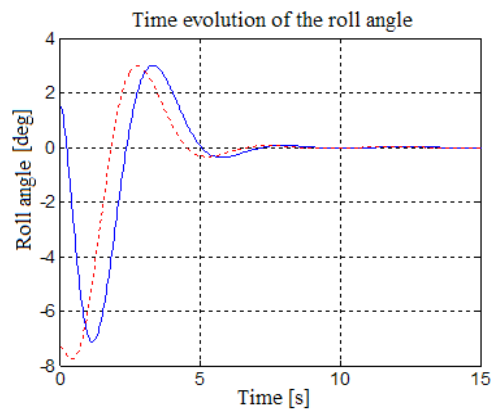


Fig.15 Time variation of the roll angle

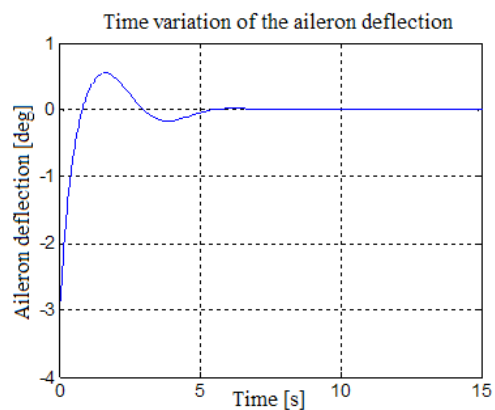


Fig.16 Time variation of the aileron deflection

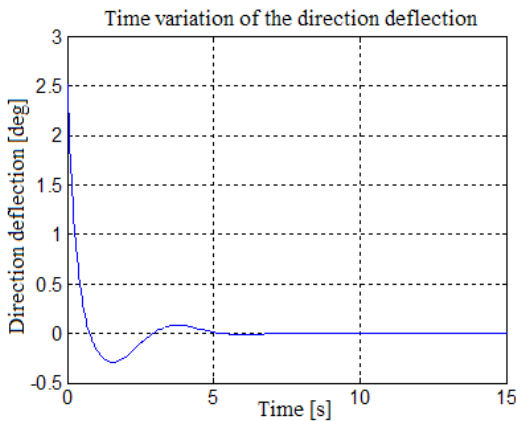


Fig.17 Time variation of the direction deflection

In fig. 18-20 one presents the Matlab/Simulink models for the blocks Eq.(25), Eq.(29) and Eq.(32) – the longitudinal movement, respectively in fig. 21-23 for the blocks Eq.(38), Eq.(43) and Eq.(46) - the lateral movement.

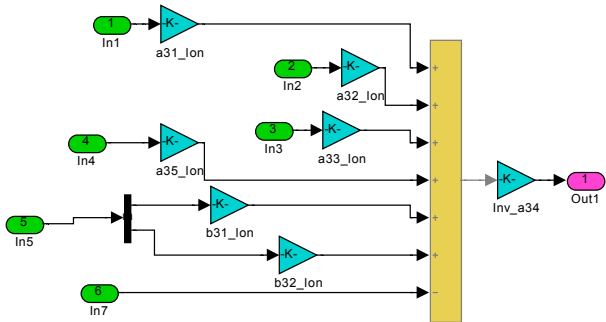


Fig.18 Matlab/Simulink model for system Eq.(25)

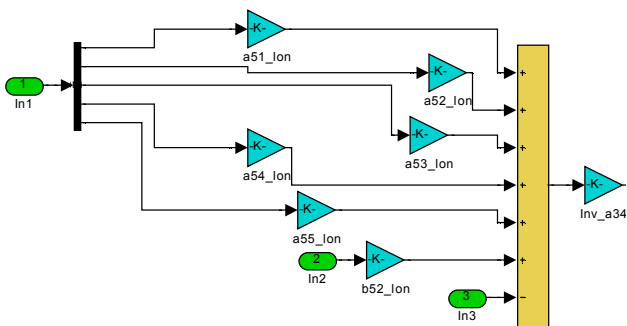


Fig.19 Matlab/Simulink model for system Eq.(29)

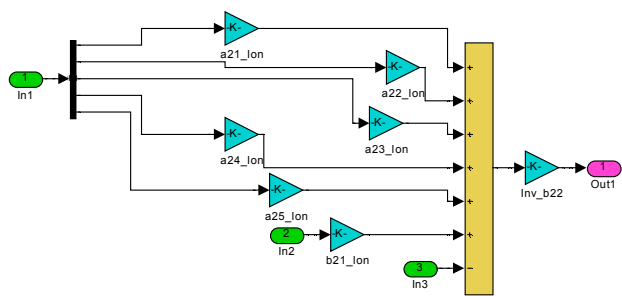


Fig.20 Matlab/Simulink model for system Eq.(32)

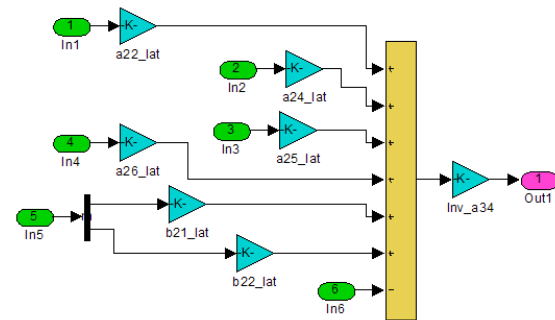


Fig.21 Matlab/Simulink model for system Eq.(38)

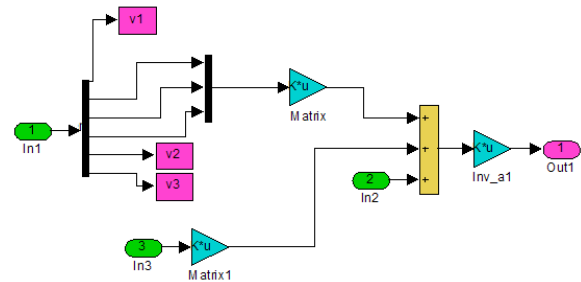


Fig.22 Matlab/Simulink model for system Eq.(43)

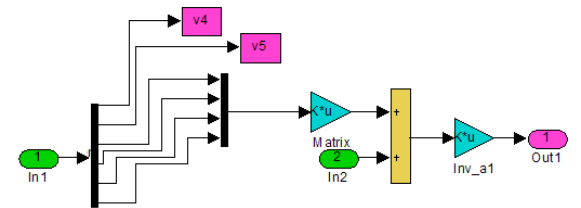


Fig.23 Matlab/Simulink model for system Eq.(46)

6 Conclusion

One knows that it is difficult to stabilize and control an aircraft using constant gain controllers because the aircraft's dynamics vary with the considerable modification of the dynamic pressure and Mach number. That's why a very good method for solve this problem is the determination of the gains of the control system. This paper presents a methodology for the flight control law's design for the trajectory pursuit using hierarchical dynamic inversion; this is based on separation of multi-time-scale and multi-loop closing method. The slow variables are controlled by the fast ones, which, in turn, are controlled by aerodynamic command surfaces. The attitude angles are taken as slow variable while angular velocities as fast variables.

The authors made the analysis of the longitudinal and lateral movements of aircrafts and obtained graphic characteristics which demonstrate the effectiveness of the proposed method.

The most efficient gain ratio between inner and

outer loop, for the longitudinal movement, is approximately 0.3 to 0.4 [1]. The authors of this paper have increased this ratio to 0.6. This way they increased the stability of the aircraft and its dynamic characteristics. Same thing is done for the aircrafts' lateral movement. In this case the authors have increased this ratio to 0.5. Same stability increasing may be observed.

7 Acknowledgments

This work was supported by the strategic grant POSDRU/89/1.5/S/61968 (2009), co-financed by the European Social Fund within the Sectorial Operational Program Human Resources Development 2007 - 2013.

References:

- [1] Fujimori A., Terui F., Nikiforuk P. Flight Control Design of an Unmanned Space Vehicle using Gain Scheduling, *Journal of Guidance, Control and Dynamics*, January 2005.
- [2] Enns D., Bugajski D., Hendrick R., Stein G. Dynamic inversion: an evolving methodology for flight control design, *International Journal of control*, Vol. 59, No. 1, 1994, pp. 71-91.
- [3] Nagash A., Enns D. Precision Approach With Curved Flight Path and Accurate Time of Arrival, *Proceedings of the AIAA Guidance, Navigation and Control Conference*, AIAA Paper 98-4207, Boston, August, 1998, pp. 1217-1223.
- [4] Bugajski D.J., Enns D. Nonlinear Control Law with Application to High Angle-of-Attack Flight, *Journal of Guidance, Control and Dynamics*, Vol. 15, No. 3, 1992, pp. 761-777.
- [5] Da Costa R., Chu Q.P., Mulder J.A. Re-entry Flight Controller Design Using Nonlinear Dynamic Inversion Controller, *Journal of Guidance and Rockets*, Vol. 40, No. 1, 2003, pp. 29-37.
- [6] Looye G., Joos H.D. Design of Robust Dynamic Inversion Control Laws using Multi-Objective Optimization, *Proceedings of the AIAA Guidance, Navigation and Control Conference*, AIAA-2001-4285, May 5, 2001.
- [7] Chelaru T.V., Pana V. Stability and Control of the UAV Formations Flight. *WSEAS Transactions on Systems and Control*, Issue 1, vol. 5, January 2010.
- [8] Zhang Y., Zhao W., Kang X. Control of the Permanent Magnet Synchronous Motor Using Model Reference Dynamic Inversion. *WSEAS Transactions on Systems and Control*, Issue 5, vol. 5, May 2010.
- [9] Yasemin I. Pitch Rate Damping of an Aircraft by Fuzzy and Classical PD Controller. *WSEAS Transactions on Systems and Control*, Issue 7, vol. 5, July 2010.
- [10] Chelaru T.V., Pana V., Chelaru A. Dynamic and Flight Control of the UAV formations. *WSEAS Transactions on Systems and Control*, Issue 4, vol. 4, April 2010.
- [11] Kemao P., Kai Y., Eng K., Dong L. Flight Control Design Using Hierarchical Dynamic Inversion and Quasi-steady States. *AIAA Guidance, Navigation and Control Conference*, 18 – 21 August 2008, Honolulu, Hawaii, AIAA 2008 – 6491.
- [12] Carlos M., Vélez S., Andrés A. Multirate control of an unmanned aerial vehicle, *WSEAS Transactions on Circuits and Systems* Issue 11, Volume 4, November 2005.
- [13] Isidori A. *Nonlinear control systems*. Springer, Berlin, 1995.
- [14] Lungu R., Bekiarski A., Lungu M., Calbureanu M. The Use of the Hierarchical Structured Dynamic Inversion to the Aircrafts Lateral Movement. *The 14th WSEAS International Conference on Systems*, Corfu Island, Greece, July 22-24, 2010.